

INVESTIGATION OF THREE DIMENSIONAL WAKE STRUCTURES OF WIND TURBINE AIRFOILS

David Francis Tidy

Supervised by Professor John Sheridan

ABSTRACT

This project investigated the three-dimensional structures present in the wake of generalised wind turbine airfoils. The research was carried out in Monash University's water channel using flow visualisation and particle image velocimetry (PIV). One swept blade and one straight blade were tested to investigate the different effects caused by a changing cross section. Both blades were subjected to three different Reynolds numbers and a range of different angles of attack. Significant three-dimensional flow was observed, including counter-rotating vortices which were of particular interest. A momentum analysis technique was utilised to calculate induced drag and local Strouhal numbers and the results were compared with literature.

INTRODUCTION

Over the last 20 or so years there has been renewed interest in wind turbines as a form of electricity generation. This has been in a large part due to the looming threat of climate change which has been mostly caused by the burning of fossil fuels for domestic energy.

As the price of producing power from wind is currently more expensive than producing from traditional sources, the wind energy industry has been investing significant resources in attempts to improve the efficiency of their turbines.

As opposed to the early windmills of the Netherlands and the farm windmills of the United States, modern wind turbine manufacturers utilise knowledge of airfoils to produce more efficient machines. Airfoil shaped blades are more efficient single element wings which is the main reason for their popularity in the design of horizontal axis wind turbines (HAWT).

To characterise the performance of airfoils, non-dimensional numbers are used such as the drag coefficient and the Reynolds number:

$$C_D = \frac{D}{\frac{1}{2} \rho V^2 A_p} \quad \text{Eq 1.}$$

$$\text{Re} = \frac{Vc}{\nu} \quad \text{Eq 2.}$$

One feature of airfoil shapes during and post stall is that they exhibit three-dimensional flow in their wakes. This three-dimensionality is embedded within the standard von Karman vortex street which sheds periodically from the trailing edge of the airfoil, often matched to the dimensionless Strouhal number. A modified Strouhal number is used in this project which is based on the projected chord normal to the freestream:

$$\text{St} = \frac{fc \sin(\alpha)}{V} \quad \text{Eq 3.}$$

Swalwell (2005, 4.3.1 p8)

Three-dimensionality has been shown to occur on the suction side of the airfoil and this implies that velocity and hence pressure fluctuations will affect the blade. Unchecked, these fluctuations could eventually destroy a blade, or, at the very least, make it less efficient.

While the most ubiquitous study of three-dimensional wake structures has been based on cylinders, a few researchers have tackled the airfoil. Schewe (2001) used oil flow visualisations to demonstrate that counter-rotating vortices appeared in fixed wavelengths across a blade depending on the flow regime. While Hoarau *et al* (2003) performed numerical simulations of flow over an airfoil with a similar result.

As the airfoil wake is predicted to behave much like that of any other bluff body, a study of literature pertaining to cylinders was also undertaken. As mentioned above, there have been many researchers involved in the study of cylinder wakes. Zhang and Dalton (1998) performed numerical simulations of cylinder wakes at low Reynolds numbers and found strong evidence of spanwise vorticity in the wake structure. This work was reinforced by Ryan *et al* (2005) who found numerically that the spanwise structures were evenly spaced.

In experimental work on cylinders, Wu and Sheridan (1994) recorded flow visualisations which clearly show counter-rotating vortices being carried downstream on the von Karman vortice sheets. Bay-Muchmore and Ahmed (1993) also produced similar images using hydrogen bubble and dye visualisation.

In investigating the causes of this circulation, Szepessy and Bearman (1992) used end effects to change the spanwise correlation of the von Karman vortice sheets. They found that the aspect ratio, as modified by the movement of end plates, had a large effect on the fluctuating lift of the blade. Szepessy and Bearman's work is also of interest in this research as the unsteady spanwise shedding of vortice sheets will necessarily create three-dimensional flow as pressure gradients develop between different sections of the blade.

With respect to the swept blade, some conclusions must be drawn from other work as it seems that the effect of sweep on a blade has not been researched before in any significant manner. From work which is analogous, Castro and Watson (2004) investigated the effect of two flat plates tapered away from one another. Also, Papangelou (1992) researched the effect of increasing the diameter of a cylinder in a spanwise direction, essentially creating a cone. Papangelou found that the von Karman vortice sheets shed the cone at a frequency determined by the universal Strouhal number at the local section of the cone. Papangelou also discovered conditions where the cone would 'try' to shed von Karman vortices at a constant frequency. As the projection of a swept blade is the same as the projection of a cone or of two tapered flat plates, it is predicted that the swept blade's wake will be analogous.

Using momentum analysis, an estimate of the induced drag due to the three-dimensional flow can be obtained:

$$D_i = \frac{1}{2} \rho \int_{-\infty}^{\infty} \int_{-\infty}^{\infty} (v^2 + w^2) dy dz \quad \text{Eq 4.}$$

Mason (2006,p5-13)

NOMENCLATURE

A_p	Planform area
c	Chord Length
C_D	Drag coefficient
D	Drag Force
D_i	Induced drag
f	Vortex shedding frequency
Re	Reynolds number
St	Strouhal number
ν	Kinematic viscosity
V	Freestream velocity
v/w	Velocity components in y/z planes
α	Angle of attack
ρ	Water density

EXPERIMENTAL METHOD

This research was conducted at Monash University's water channel on the Clayton campus. The decision to test the airfoils in water was made because flow visualisation is simpler in water and also because particle image velocimetry had been conducted there in the past. The study was performed on a NACA0021 airfoil which is a simple uncambered cross section. (Abbott & von Doenhoff, 1959)

In order to investigate the behaviour of the airfoil wakes under different flow regimes flow visualisation and particle image velocimetry (PIV) were used. Flow visualisation was used initially to gain a qualitative idea of the flow structures and the conditions under which they form. PIV was used after this to focus on areas identified by the flow visualisation work as worthy of further investigation.

Flow visualisation is a non-invasive method of recording a flow regime through a certain plane. In this case, the plane of interest was 1.5 chord lengths downstream of the airfoil looking back towards the airfoil. To achieve this visualisation, lamps were set up underneath the channel and were fitted with slotted lens covers which produced a thin light sheet. With the channel seeded with 16µm glass particles, the light sheet illuminated a plane which was then captured using a Sony HandyCam digital video camera.

Angles of attack from 0° to 90° in 3° increments were captured for the straight blade while the swept blade was captured at just one. This work gave an excellent idea of the basic characteristics of the circulation and where it occurs. To investigate this further and to produce more quantitative data, PIV was used.

PIV or particle image velocimetry works by cross correlating two images to determine a flow's velocity field at a particular point in time (Stanislas, 2000). To achieve this, two images are taken by an 11 megapixel digital camera separated by a known timestep. The timestep was 20ms in the case of these experiments. The illumination of the region of interest was supplied by two Neodymium-doped Yttrium Aluminium Garnet lasers. These lasers were pulsed 20ms apart and the laser beam was reflected 90° through a mirror and then scattered into a light sheet by a small radius lens. The firing of the camera and of the lasers was performed by a timing box. The timing box was triggered by a TTL (5V) clock signal at a constant frequency. After the timing box was started, the camera was triggered and then the laser pulses were timed to match the camera exposures.

After the PIV images were taken, they were post-processed by software developed by a Monash University academic. The output was in the form of matrices which can be imported into Tecplot or Matlab for further investigation.

RESULTS

Flow Visualisation

Significant spanwise vorticity was observed through all Reynolds numbers and through angles of attack from 6° to 90° . The spanwise vorticity appeared to be sporadic and inconsistent in both its position and strength. As the angle of attack was increased towards 90° the structures became more common, however they remained mostly unpredictable. The higher Reynolds numbers seemed to increase the probability of a counter-rotating vortice pair but also were harder to observe as the video camera frame rate was too slow to accurately resolve the particles.

Noticeably, the von Karman vortice sheet was often uncorrelated across the span. This out-of-phase shedding was visible at all but the lowest angles of attack of 0° to 6° . At other angles of attack the frequency of shedding would appear to be different at different parts of the blade. This was especially evident on the swept blade.

Particle Image Velocimetry

PIV analysis allowed a significant increase in the amount of data which could be extracted. Although counter-rotating vortices were sporadic, enough data points were captured to allow many different instances to be captured. As there is far too much data to present here, a few interesting cases will be discussed.

Firstly, a pair of counter-rotating vortices is shown in figure 1. These vortices are typical of the sort of behaviour which this research was focused on and are consistent with the findings of Schewe (2001) and others. It consists of two areas of circulation which occur in opposite directions. The linear spacing is around 40mm.

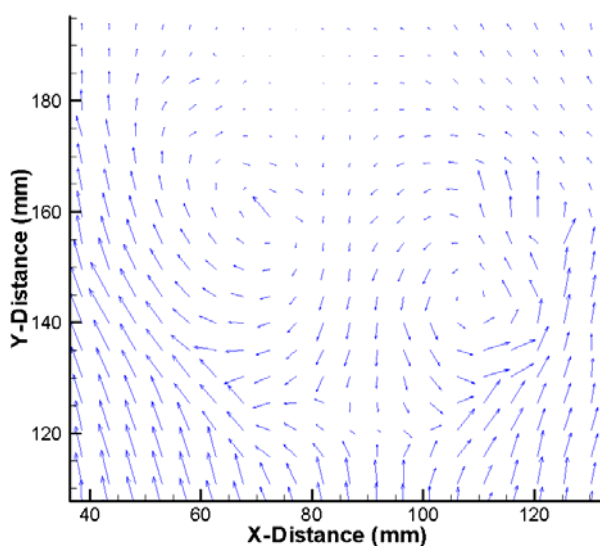


Figure 1 - PIV vector plot - 60° Re=4128

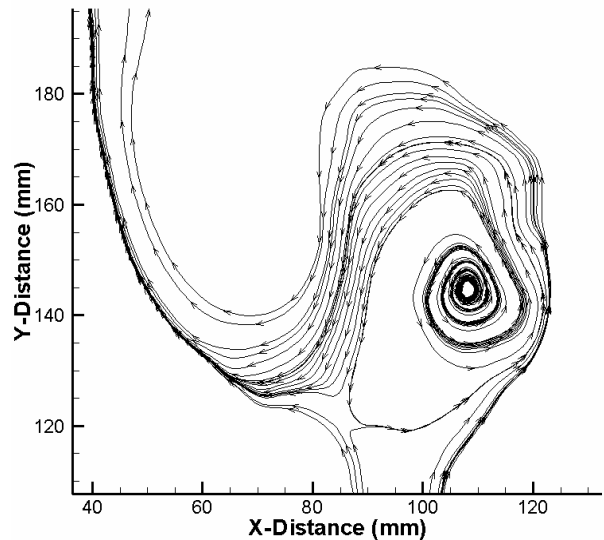


Figure 2 - PIV streamline plot - 60° Re=4128

Streamlines, are generally used for illustrating data when the structure being shown is in the same plane as the freestream. In this case, with the freestream at 90° (out of the page), it's not strictly correct to use streamlines as the particles are moving out of the page and hence cannot follow the streamline shown. However, streamlines present the information in the vector plot in a much more accessible manner. What is obvious from the streamline plot in figure 2 is the difference in strength between the left and right vortices. A possible explanation for this comes from the vector plot (figure 1). What is evident from the vector plot is that the von Karman vortice sheet, which is rolling up in front of the viewer, is stronger on the left hand side than the right hand side. This appears to have an effect on the structure of the vortice and seems to reduce its intensity. This behaviour was observed multiple times in this experimental work.

It seems as though the unsteady shedding of the vortex sheet from the trailing edge has an effect on the spanwise circulation observed at two chord lengths downstream from the bluff body. Whether it has a damping effect, or whether it could even act as a catalyst for the creation of some vortices remains to be seen. From the images recorded in this research, both would appear to be somewhat true. In particular, the images below (figures 3 & 4) may indicate this.

As mentioned earlier, the irregularity of the von Karman vortice sheets occasionally brought about a situation where two sheets would be shed with opposite rotations right next to each other. By the time they reach the viewers position, they appear as an upsurge of flow adjacent to a downsurge of flow as pictured in figure 3. Whether the shear between the two different flows caused this structure is hard to determine. However, like the previous case, it appears as though the sheet is having some effect on the three-dimensionality of the airfoil wake.

Once again, a streamline plot is presented in figure 4 as it quite clearly shows the upsurge of flow on the left and the downsurge of flow on the right. In-between

there appears a strong vortex which does not have a partner on either side.

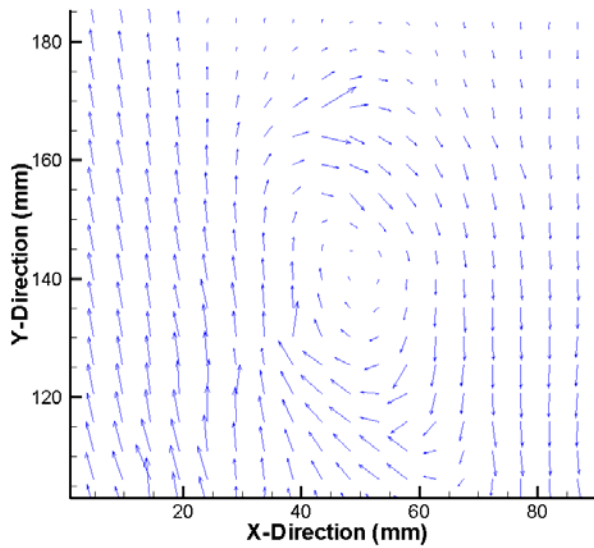


Figure 3 - PIV vector plot - 75° Re=4128

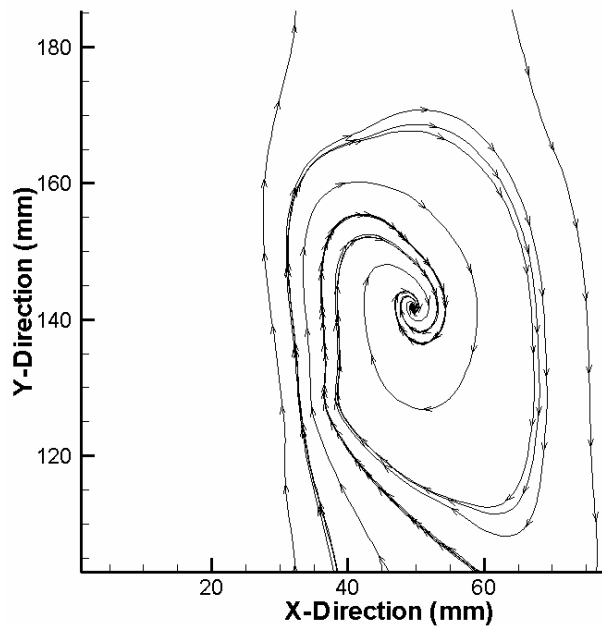


Figure 4 - PIV vector plot - 75° Re=4128

The following structure also links the von Karman vortices to spanwise circulation creation and/or destruction. The vortices captured here (figures 5 & 6) are interesting as they were captured in two successive images. In the first image (figure 5) the counter-rotating vortices are quite clear. Just above the vortices, the downsurge of a vortice sheet is also evident. By the second image, which was taken a third of a second later, the two vortices have been carried upwards by a new surge in the vertical direction, they appear to have been reduced in strength by the vortice sheet.

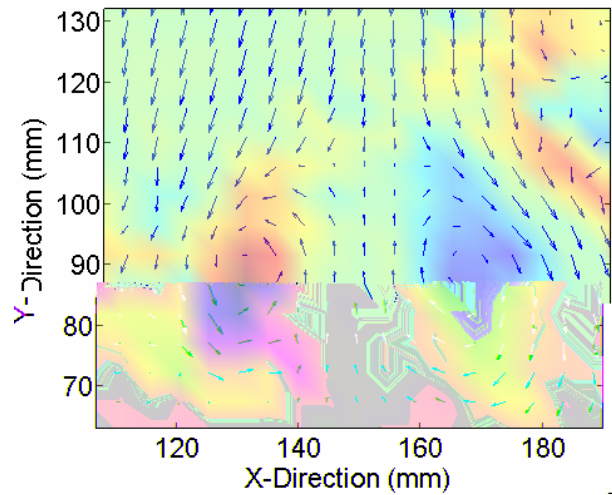


Figure 5 - PIV vorticity contour plot - 60° Re=4128

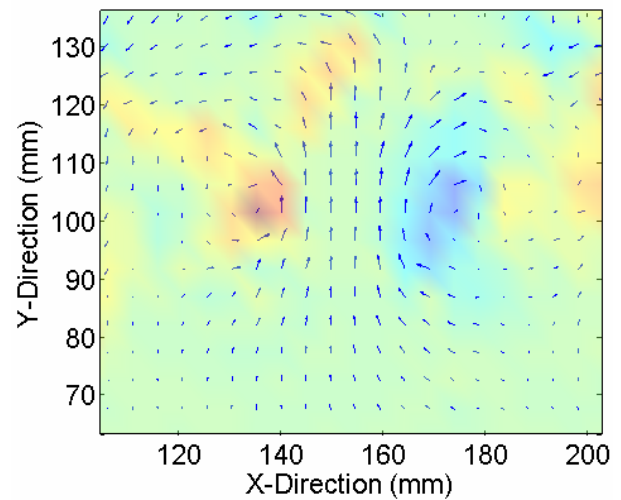


Figure 6 - PIV vorticity contour plot - 60° Re=4128

Total Circulation

As seen by Eq. 4 above, knowledge of the velocity field in this plane can be used to approximate the total drag on a body. Also, individual vortice structures can be focused on to ascertain their contribution to the total drag value.

A Matlab routine was written that would create a piecewise integral that would be solved over the entire region captured by the PIV data. Using this routine, every velocity field captured was processed and a value for drag obtained. With 20 double images captured at each angle of attack, sufficient data was available to gain reasonable averages and some interesting features were uncovered using this analysis.

For each angle of attack, using the drag information gathered from all 20 images, an average value for drag was calculated. This was non-dimensionalised to a drag coefficient based on the wing area captured in the PIV data. This led to an average drag coefficient for all 7 angles of attack over 3 Reynolds numbers. The result is a well correlated relationship:

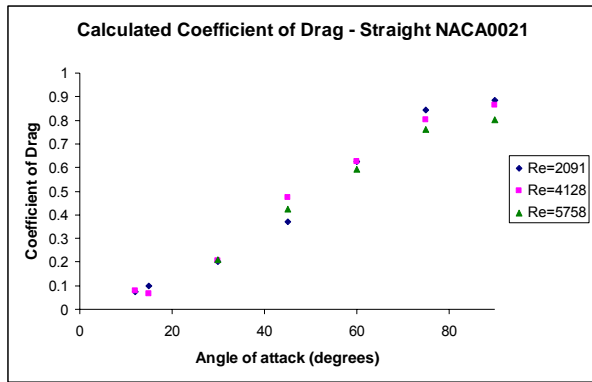


Figure 7 - Calculated drag coefficients versus angle of attack for three different Reynolds numbers

As most work in the area of drag on airfoils is performed at higher Reynolds number, the lowest published data available was for a NACA0021 airfoil at $Re=20,000$. Ward (1931, fig8) published a drag coefficient for an angle of attack of 30° of 0.3. For a 90° angle of attack, the most reasonable comparison is with a half-cylinder or a flat plate which have drag coefficients between 1.2 and 2.0 for $Re=10^4$ (White, 1999, p458) (Lam, 2005). While a little high, these figures compare fairly well with the data presented in figure 7.

Considering a freestream velocity vector does not contribute any spanwise velocity to the integral in Eq. 4, a slowing of the freestream at any point will not be recorded using this technique. Possibly the underestimation of the drag coefficient in this research is due to the lack of this freestream information captured in the PIV data.

Figure 8 demonstrates a time series calculated values for drag. Clear periodicity is shown for these angles of attack. The frequencies of this motion can be derived from the graph. Using the modified Strouhal number (Eq 3.) which uses an estimate for the wake width based on the chord length normal to the freestream, the following Strouhal numbers can be calculated:

$$St_{45^\circ} = \frac{\frac{3}{7} \times 0.045 \times \sin(45^\circ)}{0.0467} = 0.292$$

$$St_{75^\circ} = \frac{\frac{1}{3} \times 0.045 \times \sin(75^\circ)}{0.0467} = 0.31$$

$$St_{90^\circ} = \frac{\frac{3}{10} \times 0.045 \times \sin(90^\circ)}{0.0467} = 0.289$$

As published data by Hoarau *et al* (2003) places the Strouhal number of a NACA0021 airfoil at 0.34 for this Reynolds number, these results are encouraging. As seen in figure 8, the data would need to be captured at a higher rate for confidence to be placed in the frequency calculated. This is possibly the source of error which sees this work underestimate the Strouhal number slightly.

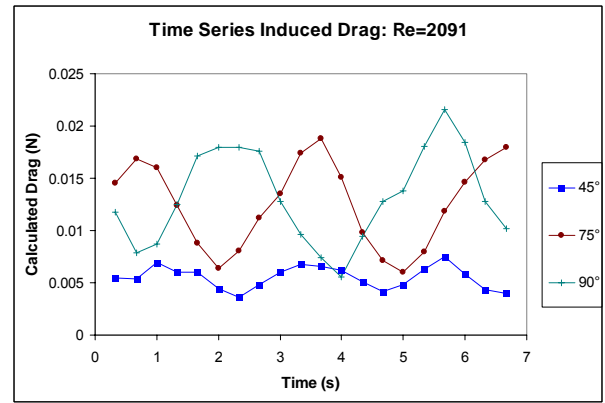


Figure 8 Fluctuating drag for $Re=2,091$

The Strouhal numbers calculated give an excellent collapse of the experimental data with the largest difference being 7.3%. With refinement and higher resolution data it's possible that this method could be as effective as pressure methods without the difficulty involved in installing pressure sensors all over an airfoil.

CONCLUSIONS

This project focussed on the three-dimensional wakes of wind turbine airfoils. Significant three-dimensional flow was observed for most angles of attack on the straight blade while the effect of the swept blade appeared to be a suppression of this phenomenon.

The counter-rotating vortices were sporadic in their appearance and impossible to predict. A couple of explanations are given:

- Aspect ratio effects allow uncorrelated vortice sheets to occur. These sheets interact with each other and possibly cause local regions of circulation to be created or damped out.
- The laser sheet could have been too far downstream which allowed instabilities to creep in and disrupt the regular and predictable counter-rotating vortices.

In this research, a more common phenomenon than counter-rotating vortices were single unaccompanied vortices. It is proposed that this is either due to one or both of the points suggested above. Or alternatively, it is suggested that the single vortice could be the result of an interaction between upsurging and downsurging vortice sheets which shear against each other.

The momentum analysis method of approximating induced drag due to the three-dimensional wake was extremely successful. This analysis allowed conclusions to be drawn on the drag coefficient versus angle of attack. The figures calculated for coefficient of drag were agreeable with published literature in the field.

In terms of the drag coefficient, the entire dataset was collapsed to a simple relationship between angle of attack and drag. The data from some 400 double images and three different Reynolds numbers produced a very satisfactory generalisation as shown in figure 7.

Similarly, the results from using the momentum equation to identify periodicity in the flow were extremely successful at generalising the dataset. Comparisons of the Strouhal numbers generated to those published in literature were successful.

With such promising results being produced using the momentum method, it is anticipated that extensive work could be performed in the future investigating the accuracy of such a method to calculate drag on various bodies. Also, the method of obtaining von Karman vortex shedding frequencies from this data is promising. It is feasible that this method could be utilised where drilling into a structure to install pressure taps is not feasible or not acceptable.

It is posited that a modified aspect ratio which would force spanwise correlation of the von Karman vortice sheets (Szepessy and Bearman, 1992) would improve the stability and predictability of the counter-rotating vortices. Possibly further work in this area could focus on this relationship between end conditions and vortice structure. In addition to this, the momentum analysis method could be compared to more traditional methods of measuring drag to assess its suitability as an experimental method.

ACKNOWLEDGEMENTS

I would like to firstly like to thank my supervisor John Sheridan for being such an inspiration, not only in this project but my entire university career.

Thank you also to Mehdi Nazarinia, Mitsushi Okada, Patrick Browne, Eric Wirth, Daniel Curtis and Andreas Fouras for being so generous with their time in helping final year students.

Thank you to Marcus Jewell, Andrew Clarke and Michael McCowan for the company during long hours in the lab.

Finally to my family, thank you for being such wonderful people.

REFERENCES

- Abbott, I. Von Doenhoff, A. (1959), "Theory of wing sections", Dover Publications, USA
- Bays-Muchmore, B. Ahmed, A. (1993), "On streamwise vortices in turbulent wakes of cylinders", *Physics of Fluids*, Vol 5, Issue 2, p387-392
- Castro, I. Watson, L. (2004), "Vortex shedding from tapered, triangular plates: taper and aspect ratio effects", *Experiments in Fluids*, Vol 37 159-167
- Hoarau, Y. Braza, M. Ventikos, Y. Faghani, D. Tzabiras, G. (2003), "Organized modes and the three-dimensional transition to turbulence in the incompressible flow around a NACA0012 wing", *Journal of Fluid Mechanics*, Vol 496, p63
- Lam, K. Leung, M. (2005), "Asymmetric vortex shedding flow past an inclined flat plate at high incidence", *European Journal of Mechanics – Fluids*, Vol 24, p33-48
- Mason, W. (2006), *Applied Computational Aerodynamics Text/Notes – Drag: An Introduction*, Class notes for AOE4114, Virginia Polytechnic Institute and State University, http://www.aoe.vt.edu/~mason/Mason_f/CAtxtTop.html, Accessed 14/10/06
- Papangelou, A. (1992), "Vortex shedding from slender cones at low Reynolds numbers", *Journal of Fluid Mechanics*, Vol 242, p299-321
- Ryan, K. Thompson, M. Hourigan, K. (2005), "Three-dimensional transition in the wake of bluff elongated cylinders", *Journal of Fluid Mechanics*, Vol 538, p1-29
- Schewe, G. (2001), "Reynolds-number effects in flow around more or less bluff bodies", *Journal of Wind Engineering and Industrial Aerodynamics*, Vol. 89, p1267-1289
- Stanislas, M. Kompenhans, J. Westerweel, J. (2000), "Fluid Mechanics and its Applications: Particle Image Velocimetry", Kluwer Academic Publishers, Dordrecht, The Netherlands
- Swalwell, K. (2005), *Effect of Turbulence on the Performance of a Small Wind Turbine*, PhD thesis, Monash University
- Szepessy, S. Bearman, P. W. (1992), "Aspect ratio and end plate effects on vortex shedding from a circular cylinder", *Journal of Fluid Mechanics*, Vol 234, p191-217
- Ward, K. (1931), *The effect of small variations in profile of airfoils*, Technical notes – National Advisory Committee for Aeronautics, No 361. Washington, USA
- White, F. (1999), *Fluid Mechanics*, McGraw-Hill series in mechanical engineering, 4th Edition, United States
- Wu, J. Sheridan, J. (1994), "An experimental investigation of streamwise vortices in the wake of a bluff body", *Journal of Fluids and Structures*, Vol 8, p621-625
- Zhang, J. Dalton, C. (1998), "A three-dimensional simulation of a steady approach flow past a circular cylinder at low Reynolds number", *International Journal for Numerical Methods in Fluids*, Vol 26, Issue 9, p1003-1022